Chapter 21

Microseismic Monitoring Developments in Hydraulic Fracture Stimulation

Mirko van der Baan, David Eaton and
Maurice Dusseault

Additional information is available at the end of the chapter

http://dx.doi.org/10.5772/56444

Abstract

The last decade has seen a significantly increased interest in microseismic monitoring by the hydrocarbon industry due to the recent surge in unconventional resources such as shale-gas and heavy-oil plays. Both hydraulic fracturing and steam injection create changes in local pore pressures and in situ stresses and thereby brittle failure in intact rock plus additional slip/shearing in naturally fractured rock. Local rock failure or slip yields an acoustic emission, which is also known as a microseismic event. The microseismic cloud represents thus a volumetric map of the extent of induced fracture shearing, opening and closing. Microseismic monitoring can provide pertinent information on in situ reservoir deformation due to fluid stimulation, thus ultimately facilitating reservoir drainage. This paper reviews some of the current key questions and research in microseismicity, ranging from acquisition, processing to interpretation.

1. Introduction

Microseismic events are very small earthquakes of generally negative moment magnitude[1] that are often associated with hydraulic fracturing or fluid flow in reservoirs. Building upon long-standing applications of microseismic methods, such as monitoring of stability in underground mines (e.g., Gibowicz and Kijko, 1994; Urbancic and Trifu, 2000)

1 Earthquake magnitude is measured on a logarithmic scale. Various roughly equivalent amplitude-based magnitude scales are in use, of which moment magnitude is the most general.

and enhanced geothermal systems (e.g., Häring et al., 2008), microseismic monitoring techniques are being used increasingly by the oil and gas industry to monitor hydraulic stimulation of "tight" (very low permeability) hydrocarbon reservoirs and steam injection into heavy-oil fields. As such, it is one of the technologies underpinning the recent upswing of oil production in Western Canada, as well as the development of new tight-gas fields, monitoring of caprock integrity during in situ heavy-oil exploitation, and carbon capture and storage (McGillivray, 2005; Maxwell et al., 2010; Verdon et al., 2010; Maxwell, 2011; Clarkson et al., 2011).

This paper reviews some of the current questions and research in microseismicity, ranging from acquisition, processing to interpretation. However, before reviewing these aspects, it is important to consider the wider context first and the economic impact of hydraulic fracturing in tight-hydrocarbon fields.

2. Background

Security of energy supplies, the continuous growth in energy demand, and climate change are among the greatest global challenges that we face. Nearly all projections agree that we will remain heavily reliant on fossil fuels for many years. For example, the International Energy Agency's 'business-as-usual' analysis from 2008 indicates that in 2030 approximately 83% of the world's energy demand will still be met by fossil fuels. In 2011 this was revised downward to 55% due to high oil prices, government incentives for renewable energies and environmental concerns (EIA, 2011). Technological innovations will therefore be required to (i) find new hydrocarbon reserves or enable recovery from proven resources previously inaccessible or uneconomic; (ii) maximize recovery from producing reservoirs, and (iii) deal with CO_2 emissions. Microseismic monitoring and hydraulic fracturing are mainly related to the first two points.

Recovery of hydrocarbons from previously uneconomic yet proven resources such as shale-gas and other tight-gas plays has become possible due to significant improvements in the last 10 years in two key technologies, namely horizontal drilling and hydraulic fracturing. Tight-gas reservoirs are characterized by low porosity and permeability, indicating that little pore space is present and that fluid flow is guaranteed to be slow and difficult, thus severely complicating reservoir drainage. On the other hand, this gas is often located in very thick lithologic units such that the resource volume is large. Horizontal drilling into these units enables drainage over a larger well contact area (2-3 km instead of 100-200m), thus improving fluid flow. In hydraulic-fracture well treatments, fluids possibly mixed with proppants (slurry) are injected under high pressure to induce fracturing of the reservoir, thereby further enhancing reservoir drainage by increasing the effective permeability through the creation of an interconnected fracture network.

The technological advances in these two key technologies have been such that in 2000 only 1% of the total gas production in the US came from shale-gas fields, whereas currently this is estimated to be 20% (IHS CERA, 2010). Figure 1 shows the extent of current and potential

http://dx.doi.org/10.5772/56444

shale-gas plays in North America. It is clear that tight-gas and shale gas will remain an important resource for many years to come and further technological improvements will enable economic drainage of additional reservoirs. One of these emerging technologies is microseismic monitoring.

Figure 1. Current shale plays in North America. Source: EIA http://www.eia.gov/pub/oil_gas/natural_gas/analysis_publications/maps/maps.htm

Hydraulic fracturing (also known as fraccing or fracking) leads to brittle failure inside a reservoir, which is typically accompanied by microseismicity. Microseismicity refers to discrete rock-deformation events, analogous to tiny earthquakes, that are generally of moment magnitude < 0. For reference, magnitude 0.2 is the equivalent of the energy released by a large hand grenade (30 g TNT equivalent), whereas a typical small mining blast has a magnitude around 1-1.5, corresponding to 2-2.5kg of TNT. Since magnitude scales are logarithmic, negative magnitude events thus correspond to the energy yield equivalent of milligrams or even micrograms of TNT.

Monitoring of microseismic activity is a geophysical remote-sensing technology that provides the ability to detect and map associated fracturing processes, either in real-time or in post-processing mode. A typical field deployment involves the installation of an array of continu-

ous-recording 3-component geophones within observation well(s) near the zone of interest, and/or a large number of surface sensors. Although relatively new to the oil and gas industry, similar monitoring technologies for earthquakes have been honed and developed by the seismological and mining research communities for decades (e.g. Gibowicz and Kijko, 1994; Bolt, 1984; Stein and Wysession, 2003). The goal of microseismic monitoring is to detect, locate and characterize microseismic events, which often occur in large numbers within cloud-like distributions that reflect underlying fracture networks. This approach enables monitoring of frac treatments in real-time in order to detect the extent of the stimulated rock volume and thus the success of the treatment, as well as predict likely improvements in subsequent reservoir drainage.

Applications of microseismic monitoring within industry, particularly in oil and gas, have seen remarkable growth during the past 10 years (Warpinski, 2009; Maxwell, 2010). This has not been limited to hydraulic fracture treatment for shale-gas and other tight-gas plays, but has included stimulation technologies such as fracturing or steam injection applied to tight-oil or heavy-oil fields and also techniques for maximizing recovery from producing reservoirs. It is estimated that over one million hydraulic fracture treatments have been performed in the US in the past 60 years (King, 2012), and that currently 3-5% of fracs in North America involve microseismic monitoring. Oil and gas companies have made significant expenditures (conservatively $100's MM) for microseismic monitoring, but face extraordinary technological challenges to fully utilize the results. Their efforts are hampered by a number of factors, including an incomplete understanding of seismological and geomechanical processes associated with induced microseismicity.

In the next sections we will review current pertinent research questions on microseismic acquisition, processing and interpretation. Since many items are intimately intertwined it is inescapable that some points may be revisited throughout the chapter.

3. Acquisition

Based on the current state-of-the-art for microseismic monitoring, a number of important technological questions are presently under debate, such as:

- What conditions favour surface versus borehole microseismic acquisition? Surface acquisition involves the deployment of large numbers of receivers and has the inherent advantage of more extensive azimuthal coverage (solid angle); in principle, this should improve the condition number for hypocentre inversion and moment-tensor analysis (Eaton and Forouhideh, 2011). On the other hand, placement of geophones in deep boreholes (currently the norm for microseismic monitoring in western Canada) has the advantage of better signal-to-noise characteristics due to the closer proximity to the microseismic sources, generally quieter background noise levels (less anthropogenic noise), often better instrument coupling and predominantly horizontal (layer-parallel) instead of vertical (layer-perpendicular) wave propagation leading to less wave scattering. Conversely, surface acquisition is significantly more cost effective as there is no need to drill observation wells

http://dx.doi.org/10.5772/56444

or deploy instrumentation inside wells, and permits deployment of one or two orders of magnitudes more instruments.

- The current strategy for hydraulic fracturing of tight-gas reservoirs is to minimize acquisition durations to reduce costs. Recently recognized phenomena, such as long-period long-duration events (Das and Zoback, 2011), indicate that much can be learned from the use of exceptionally long deployment times (i.e., weeks rather than days) in order to enable more complete characterization of background noise spectra. Such long recording durations would also enable the evaluation of technology for noise interferometry (cf. de Ridder and Delinger, 2011) to reveal not only what happens during stimulation, but also in the period before and immediately following the slurry injection.

- Various formulas are currently used within industry to calculate the magnitude of microseismic events (Shemata and Anderson, 2010). Since magnitude formulas were developed for describing earthquake phenomena, they are calibrated for significantly larger magnitudes. The extrapolation of different formulas to 4-5 orders of magnitude below their calibration range leads to discrepancies in reported values. Accurate magnitude determination is of practical importance for various reasons, including (i) the determination of the stimulated rock volume (Maxwell et al., 2006); (ii) recently implemented controls in the UK on hydraulic fracturing operations are based on a "traffic-light system" (de Pater and Baisch, 2011) in which operations are suspended for several days if any event exceeds ML = 0, and stopped if any event exceeds ML = 1.7; and (iii) on liability issues related to induced seismicity (Cypster and Davis, 1998).

- Currently the emphasis is on mapping brittle failure, yet it is hypothesized that the cumulative energy released via brittle failure represents only a minute fraction of the total injected energy, indicating that a large portion of energy release may occur aseismically (i.e., plastically or at very slow deformation rates) (Maxwell et al., 2009). This suggests that there may be an advantage to acquisition of continuous recordings for analysis of the ultra-low frequency spectral content of microseismic activity, which may be diagnostic of certain types of aseismic rock failure (Benson et al., 2008; Pettit et al., 2009; Beroza and Satoshi, 2011).

A university-led project to acquire microseismic data was undertaken in northern British Columbia, Canada. This experiment involved the recording of several multistage hydraulic fracture treatments performed in two horizontal wells (Figure 2). The microseismic data were collected using both surface and borehole sensors. The borehole tool string consisted of a 6-level broadband system with downhole digitization. Surface sensors included a 12-channel array with a mix of vertical-component and 3-C geophones, and 22 broadband sensors deployed in 7 localized arrays over an area of ~ 0.5 km^2.

The unusual setup was designed to investigate multiple objectives. First, microseismic monitoring was performed using both surface and borehole equipment to compare acquisition strategies and determine their respective advantages and inconveniences such as ease of deployment, costs, detectability of events, other signals and associated noise levels. In addition, the experiment is unique in that both broadband and short-period equipment are deployed. The approximate lowest recording frequencies for the various equipment are; broadband

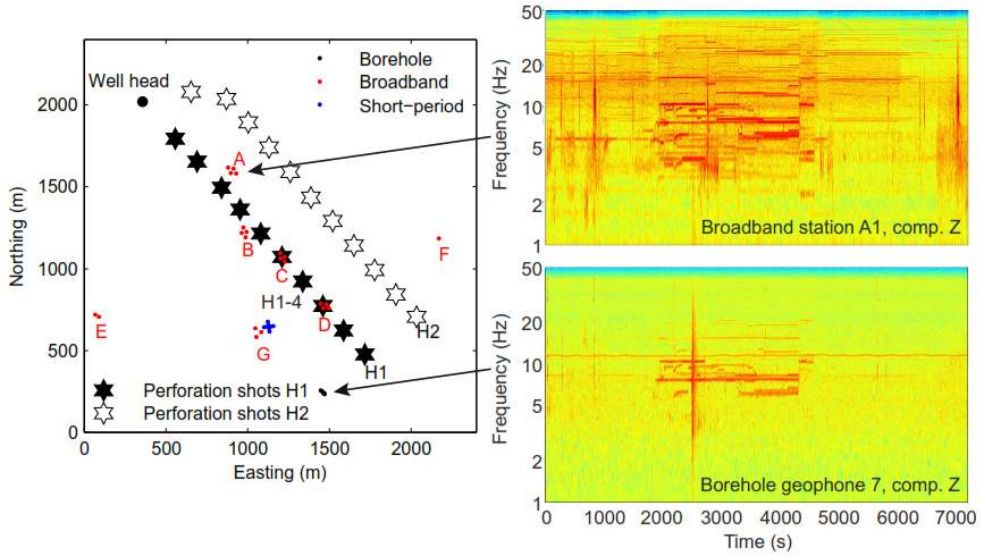

Figure 2. Experimental setup of the microseismic experiment, as well as the time-frequency transforms of stage H1-4 for one downhole geophone and one broadband station (hot colors correspond to high amplitudes). The stars indicate the position of the perforation shots and hence of the horizontal part of the wells. H1 and H2 are two different horizontal wells. After: Tary and Van der Baan (2013).

surface-based seismometers: 0.0083 Hz (= 120 s); borehole equipment: 0.1 Hz; short-period surface array: 5 Hz. Data analysis of the variously recorded signal thus helps reveal if significant energy is present below the 5 Hz limit imposed by most standard monitoring equipment. This may help resolve the observed energy imbalance between injected and seismically released energy.

Conventional analysis of microseismic recordings involves first identifying and extracting individual events, e.g., via a semi-automatic triggering system. This poses problems if many overlapping events are simultaneously recorded and if individual event strengths hover around the noise level. It also may obscure proper identification of so-called slow earthquakes (Ide et al., 2007) occurring on much longer time scales than conventional earthquakes resulting from abrupt brittle failure.

Direct analysis of continuous data streams on the other hand offers much greater flexibility and is not subject to the shortcomings described above. For instance, analysis of continuous recordings of acoustic emissions generated during laboratory rock-fracturing experiments have greatly aided in improving our understanding of active microcracking and deformation processes in volcanoes and the earth in general (Benson et al., 2008; Thompson et al., 2009). These continuous data streams are analyzed using various time-frequency transforms such as short-time Fourier transforms, S-transforms and wavelet transforms (Reine et al., 2009) to examine variations in local frequency content and highlight

http://dx.doi.org/10.5772/56444

slow deformation processes. Obviously it remains possible to dissect the recordings to extract individual events as well.

Initial analysis of these data reveals the existence of numerous high-frequency (> 100 Hz) microseismic events with moment magnitudes ranging from -2.3 to -1.4. These events are detected to distances of up to 1.2 km using the borehole system. In addition, perforation shots are well recorded to distances of about 2 km. More interestingly spectral analysis shows the existence of complex rupture patterns such as rapid opening and closing of tensile cracks (Eaton, 2012). Moment tensor analysis on other experiments has shown complex deformation as well in hydraulic-fracturing experiments (Baig and Urbancic, 2010); yet such moment-tensor analysis normally requires two or more observation wells (Eaton and Forouhideh, 2011). The current observations are obtained using a single observation well.

Time-frequency analysis of the continuous recordings demonstrates the existence of resonance frequencies during hydraulic fracturing (Tary and Van der Baan, 2013). The resonances are mainly in the frequency band between 5 and 20 Hz. Other resonances are visible on the broadband recordings. They likely correspond to environmental or anthropogenic noises. Noticeably, the resonances are recorded by the downhole geophones, which are close to the horizontal part of the injection well at depth, and by the broadband arrays A and B, which are near the well head. The broadband arrays C or D, closest to the fluid injection during the first stages, do not exhibit any resonance frequencies. This indicates that the injection well is likely the cause of these resonance frequencies (Figure 2). In other cases, however, resonance frequencies may be indicative of the extent of the induced, interconnected fracture network (Tary and Van der Baan, 2012).

It is clear from the above discussion that many key acquisition questions are intimately linked to the need to enhance our arsenal of tools for processing and interpretation of microseismic data.

4. Microseismic data processing

Rapid turnaround has been a high priority within the microseismic industry to reduce acquisition durations and deliver analysis results such as event locations in near real-time to completion engineers, who are required to make decisions such as starting a new fracturing stage based on assessment of a microseismic event “cloud” distribution. This requirement has led to the development of near real-time event-picking, classification and hypocentre-location algorithms; such rapid turnarounds demand robust techniques based on straightforward assumptions, often accompanied by large reductions in information content. For instance, in the case of hydraulic fracture stimulations, the fracture size and orientation are often inferred using a few events comprising the edges of the “cloud” of microseismic hypocentres.

4.1. Analysis and attenuation of coherent noise

Before discussing picking and event location it is important to realize that a principal aspect of microseismic data processing is the recognition and attenuation of coherent noise. Coherent noise is defined here as any repeatedly recorded energy on one or more traces that is not a body wave (P or S) arrival. The noise is often persistent, repeatable, and may be caused by various types of waves travelling in the borehole. A cemented wellbore with steel casing has the potential to propagate many types of waves. P and S waves can be transmitted in a wellbore in the steel casing, or the cement (Raggio et. al., 2007). The P wave can also be transmitted in the fluid in the wellbore. There are also a number of modes of tube waves (Rayleigh waves travelling at the wellbore fluid and adjacent solid interface) that can be transmitted.

St-Onge and Eaton (2011) have observed another type of coherent noise source that may be related to the tuned response of a clamped geophone array. This response is manifested as discrete, high-amplitude spectral peaks that can have a negative effect on weak signals recorded within the primary bandwidth of borehole microseismic recordings (i.e., several hundred Hz). These observations show that noise can be high in amplitude, persistent in time, and may adversely affect the recording of P and S wave signal energy in microseismic data (St-Onge and Eaton, 2011). Due to the nature of the data acquisition, the types of noise observed in microseismic surveys differ from typical noise sources in conventional seismic profiling. In many cases, datasets are contaminated by Lamb waves, which are a type of elastic guided wave that travels along a plate surface such as the cylindrical surface of borehole casing. These coupled longitudinal and transverse waves were first described by Lamb (1917) and in a cylindrical casing exhibit longitudinal, torsional and flexural modes. Lamb waves are dispersive, and their frequency characteristics have been described by Karpfinger (2009). St-Onge and Eaton (Lamb waves recorded in wellbores and their potential to predict cement bond failure, in preparation for Geophysics) are exploring various ways in which these harmonic signals can be suppressed or even exploited to characterize the borehole environment as their propagation velocity is influenced by the bonding characteristics of the cement.

Tary and Van der Baan (2012) divide resonance frequencies into three broad categories, namely those generated by source, receiver or path effects. This categorization can also be applied to microseismic noise if we are interested solely in the microseismic direct arrivals for location purposes and estimation of the associated source mechanism. At the receiver side, resonance frequencies and other noise result from wave reverberations in the borehole (Sun and McMechan, 1988), either the whole borehole or between secondary sources such as the geophones (St-Onge and Eaton, 2011). Resonances and noise can also be due to internal resonance of the geophone if its clamping or damping is flawed.

Along the ray path, resonances arise from constructive and destructive interferences of seismic waves, waves focusing in low-velocity waveguides or multiple wave scattering. Which frequency band is favored depends on the layer spacing, thickness and mechanical properties (van der Baan et al., 2007, van der Baan, 2009). Likewise (multiple) reflections and refractions can also confound the picking of direct arrivals. A prime example on how such secondary arrivals can complicate event picking and location is shown in Kocon and Van der Baan

http://dx.doi.org/10.5772/56444

(2012) who demonstrate that mis-identification of arrivals is a prominent source of event mislocations.

At the source side, resonance frequencies can be generated by repetitive events if perfectly periodic, or by the resonance of fluid-filled cracks as in the case of volcanic tremors (Aki et al., 1977). Resonances in fluid-filled cracks are generated by interface waves and depend mainly on the crack geometry, the crack stiffness and the source parameters that trigger the resonance (Ferrazzini and Aki, 1987). The latter are significantly less likely to mask strong direct arrivals; yet they offer promise for enhancing our understanding of the geomechanical reservoir deformations during hydraulic fracturing (Tary and Van der Baan, 2012, 2013) as indicated in the previous section.

4.2. Traveltime picking

Event-detection and time-picking are critical steps for microseismic data processing. Due to the large volume of data acquired during a microseismic survey, these steps are typically performed using an automated method. These steps have been implemented using various algorithms, such as the short- and long-time average ratio (STA/LTA) technique (e.g. Sharma et al., 2010), modified energy-ratio (MER) (Han et al., 2009) and Akaike information criterion (AIC) (Oye and Roth, 2003). Akram et al. (Automatic event-detection and time-picking algorithms for downhole microseismic data processing, manuscript in preparation for Geophysical Prospecting) have developed a dynamic-threshold approach for event detection that reduces false detections and offers improved capability to identify weak signals. They have also developed several hybrid approaches for automatic arrival-time picking that combine existing methods to improve performance with real microseismic data.

4.3. Locations

Calculation and interpretation of the locations of seismic events (hypocentres) are critical first-order components of microseismic monitoring. Compared to conventional earthquake methods, borehole microseismic surveys are relatively poorly constrained because of the fewer number of geophones and less desirable azimuthal coverage (Han, 2010; Jones et al., 2010). Most hypocentre localization methods require knowledge of P- and S-wave arrival times (Xuan and Sava, 2009). For borehole microseismic surveys, the distance between source and receiver can be computed using the arrival time difference of P- and S- waves and azimuth and dip information obtained from polarization analysis (Albright and Pearson, 1982; Eisner et al., 2009; Han, 2010; Jones et al., 2010). A probability density function can also be computed from the observed and modeled arrival time delays of P- and S-waves (Michaud et al., 2004). Surface microseismic methods are better suited to migration-based methods, which do not require P- and S-wave arrivals time picking information and can locate weak events by focusing energy at the source using time reversal (Gajewski, 2005; Chambers et al., 2009; Fu and Luo, 2009; Xuan and Sava, 2009). The drawbacks of the migration-based methods include high computational cost and their requirement of data redundancy (Xuan and Sava, 2009; Han, 2010). A semblance-weighted stacking method can also be used for microseismic source location, where the maxi-

mum value of the product of P- and S-wave semblances on a time window define the location of microseismic source (Eaton et al., 2011).

There are also several techniques (for example, hypocentroidal decomposition and double-difference tomography), which determine the relative location of the seismic source (Shearer, 1999). It has been recognized that the near real-time hypocentre locations may have large associated uncertainties, preventing high-resolution post-treatment interpretation (Figure 3). A first concern is that different service companies may obtain different event locations, even for the same dataset. This is caused by fundamental uncertainties in how to determine the most appropriate velocity model, the use of different event location algorithms but also elemental problems on how to pick consistently P- and S-wave arrivals in large datasets (sometimes consisting of 1000s of events recorded by 10s or 100s of 3-component receivers).

Much current research focuses on improved workflows for direct estimation of absolute hypocentres and on accurate relative event locations. Multiplet analysis can for instance be used to address the issues of unknown velocity models as well as inconsistent picking on final event locations (De Meersman et al., 2009; Kocon and Van der Baan, 2012). A doublet is a pair of events produced by nearly identical source mechanisms from closely spaced locations; a multiplet is a group of three or more of such events. The waveforms of multiplets are nearly identical, with the principal exception of additive random noise. Multiplets can be readily identified using cross correlation (Poupinet et al. 1984; Arrowsmith and Eisner, 2006). All events in each multiplet group are then relocated to improve their relative location accuracy (Figure 3), thereby revealing lineations and active faults planes.

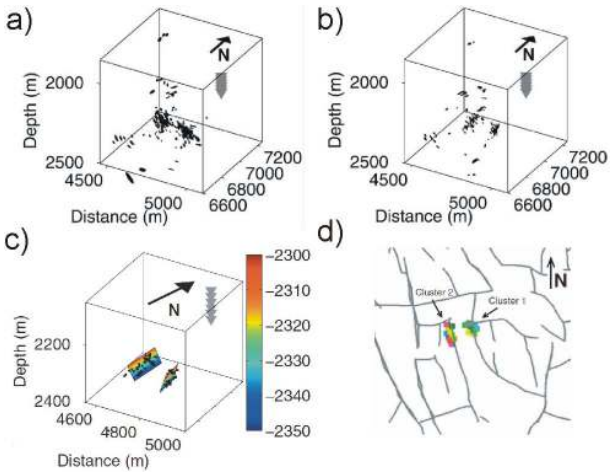

Figure 3. Microseismic events contain a wealth of information that can be used to determine planes of weakness along which fluid migration could occur. (a) Original source locations; (b) new source locations after application of a high-resolution relocation technique; (c) multiplets extracted and best fault plane solutions depicted in two major clusters; (d) obtained fault planes overlain onto the top-reservoir fault map interpreted from 3D surface seismic data (after De Meersman et al., 2009).

http://dx.doi.org/10.5772/56444

This approach has two important advantages. First the method is rather insensitive to the chosen velocity model since any inaccuracies will not obscure revealed geologic features but only change their size (Got, 1994, De Meersman et al., 2009). Secondly, mispicks and missing picks are automatically corrected for via the cross-correlation procedure. In addition, a crossplot of waveform correlation coefficients versus hypocentre separation distances of every event pair automatically reveals hypocentre location errors by examining location distances of identified multiplets. This technique enabled Kocon and Van der Baan (2012) to ascertain that events could be mislocated by 350m in a heavy-oil dataset due to erroneous traveltime picks.

Once the multiplet groups are detected, the double-difference method can be applied. This is a relative relocation method that seeks to reduce the effects of errors due to unanticipated velocity heterogeneities in the structure (Waldhauser and Ellsworth, 2000). An advantage of this method is that no master event is needed, which induces spatial limitations, since all events must be correlated with the reference event. The main assumption in this method is that ray paths between two events will be very similar if their hypocentral separation is small compared to the source-receiver distances; therefore, the relative travel-time difference at a common station will be mainly due to the spatial offset between both events. In other words, the effects of most velocity heterogeneities will cancel out, such that only knowledge of the velocities in the source region is required. Castellanos and Van der Baan (2012) apply this method to data from a mining environment. Results clearly reveal a linear feature after relocation, possibly related to horizontal drilling activities.

Likewise, De Meersman et al. (2009) use relative locations to delineate a graben-like extensional structure in the caprock of a producing reservoir in the North Sea, UK (Figure 3). This graben-like structure was not visible in the original absolute locations which revealed solely two large microseismic clusters. Next they re-examine temporal changes in anisotropy as found by Teanby et al. (2004a) using the automated shear-wave splitting methodology of Teanby et al. (2004b) for this same dataset. They then argue that their integrated analysis of relocated sources, seismic multiplets, and S-wave splitting supports a model whereby stresses in this reservoir recharge cyclically. Effective stress builds up in response to reservoir compaction as a result of oil production, and stress is released by means of microseismic activity once criticality is reached on slip planes. These changes cause variations in seismic anisotropy and the microseismic source mechanisms over time.

5. Better understanding of physical processes associated with microseismicity

The microseismic case studies by De Meerman et al. (2009) andCastellanos and Van der Baan (2012) do not include fluid injection; yet they already demonstrate that analysis of the microseismic cloud of event locations can reveal important insights into the local geology and subsurface deformations. Pore pressure and stress changes during hydraulic fracturing lead to a propagating cloud of microseismic events, which can be recorded and analyzed to

constrain the volume of the stimulated zone. Because pressures and stresses diffuse/propagate beyond the fluid-filled fractures and affect the (generally jointed) rock mass in all directions, the microseismic cloud represents a volumetric map of the extent of shear and opening of naturally fractured rock.

A key element in current research is to develop interpretation methods that bridge the gap between geophysical data analysis and engineering applications of microseismic data. Ultimately, operators would like to know how to optimize the fracturing treatment given the in situ stress regime, dominant natural fracture orientations, pre-existing faults and other zones of weaknesses, and the prevailing lithologies. Phsyically, there exists an intimate link between the above geologic features, employed stimulation strategies and resulting microseismicity. Existing unknowns can be summarized using the following two fundamental questions: (1) Given a known stress field, geology, rock mass fabric and injection strategy, what are the most likely resulting microseismic characteristics (e.g., hypocentres, source mechanisms and magnitudes)? (2) What does measured microseismicity reveal about the existing stress field and local geomechanical properties of the rockmass? The first question involves solving the forward model (given the physical parameters, what are the resulting observations?) The second question involves solving the inversion problem (given our observations, what can we determine about the current physical state?).

From an engineering point of view, answering these questions will have an immediate impact on first creating optimal drainage and fracturing strategies and then confirming their success or failure prior to starting production. From a geophysical perspective, recorded microseismicity and integration of the results with surface seismic data should significantly enhance our understanding of the existing subsurface geologic conditions and the geomechanical behavior of the reservoir, thus providing pertinent information to the completion engineers.

Pertinent considerations include: (1) Obtaining accurate locations for microseismic events to support meaningful volumetric analysis of the associated microseismic cloud. (2) Inferring the failure mechanism (i.e., are fractures opening, closing or shearing?). (3) Determination of why failure is occurring in specific locations but not in others (why are fractures not always symmetric with respect to the injection well and what is the geomechanical behavior of the reservoir)? The last question, in particular, is difficult to answer from the recorded seismicity alone since the geomechanical behavior depends on the in-situ stress field, the local rock properties (lithologies), and any existing areas of weakness including faults, fractures and joints (Grob and Van der Baan, 2011, Chorney et al., 2012).

5.1. Advanced microseismic source analysis

Robust characterization of microseismic sources has the potential to provide important information about deformation mechanisms. Borrowing from earthquake seismology, seismic moment tensors can be used to describe microseismic point sources in general terms of a set of force couples. Moment tensors can be represented in terms of source type (Hudson et al., 1989), a classification scheme that includes shear slip (double couple), dipole, compensated linear vector dipole and volumetric sources. The reliability of these classification schemes depends critically upon the use of a recording array with a suitable geome-

http://dx.doi.org/10.5772/56444

try that satisfies geometrical requirements for azimuthal coverage of the source region (Eaton and Forouhideh, 2011).

Other fundamental descriptions of microseismic sources include the seismic moment and associated energy release, in addition to spectral source characteristics that reveal the time- and spatial-scales of rupture. Recent developments in earthquake seismology suggest that rock-deformation processes commonly occur across a broad spectrum of time scales (and frequency), wherein earthquakes merely represent a high-frequency end member (e.g., Beroza and Ide, 2011). We postulate that rock deformation processes associated with hydraulic fracturing obey scaling laws that are similar to earthquakes. If so, microseismic activity recorded conventionally using geophones, which are relatively insensitive to ground motion below their natural frequency (typically ~ 10 Hz), could represent a high-frequency end member of the complete deformation spectrum.

Seismic moment-tensors provide a general mathematical representation of seismic point sources (Ben-Menahem and Singh, 2000). Inversion techniques to estimate moment tensors from seismic recordings are well developed in earthquake seismology, but are only starting to be used in microseismic monitoring applications (Baig and Urbancic, 2010). The determination of moment tensors can potentially provide useful insights into rupture processes, but care is required to ensure that survey design is adequate (Eaton and Forouhideh, 2010; 2011).

The spatial dimensions of microseismic events are encoded in the spectra of the radiated seismic waves. Microseismic events can therefore be analyzed using spectral methods (e.g. Eaton, 2011), providing an alternative approach for characterizing sources. For example, models for shear slip on a circular crack (Brune 1970, 1971; Madariaga, 1977) predict the shape of source spectra and provide scaling relationships between spectral parameters and source parameters (slip area and seismic moment). These source attributes complement those derived from moment-tensor inversion.

Tensile microseismic events are believed to play an important role during hydraulic fracture treatment of unconventional reservoirs (Baig and Urbancic, 2010). Tensile microseismic events may be associated with self-propping (remnant aperture), or wedging open of natural fractures because of the induced strain field. Walter and Brune (1993) developed a model for far-field source spectra for tensile rupture, and compared these with modeled far-field spectra for shear-slip events and showed that anomalously low S/P spectral amplitude ratios are a diagnostic characteristic of tensile rupture. Building on this approach, Eaton et al. ("Scaling relations and spectral characteristics of tensile microseisms", manuscript in preparation for Geophysics) investigate source characteristics of microseismic events induced by hydraulic-fracturing, with application to microseismic data from the previously described multistage treatment in northeastern British Columbia. They show that although spectral estimates of magnitude are relatively unaffected by uncertainty in seismic attenuation, for typical microseismic magnitudes accurate knowledge of seismic attenuation is necessary to estimate some spectral parameters. They also document microseismic events with spectral characteristics that reflect a complex rupture pattern, such as rapid opening and closing of tensile cracks.

5.2. Geomechanical response and reservoir analysis

As indicated above, the reliability with which moment tensors can be determined depends strongly on the acquisition geometry (Eaton and Forouhideh, 2010; 2011). There is thus a need for alternative and complementary analysis methods to reveal more about the in situ stress field. Fortunately, independent information on the in situ stress field can also be obtained by analyzing the frequency-magnitude distribution of microseismic events. This is achieved by plotting the distribution of event magnitudes on a semi-log plot (Figure 4). This distribution, also called the Gutenberg-Richter relation, usually shows a power law behavior. Its linear slope gives the so-called b-value. Schorlemmer et al. (2005) have shown that this b-value changes depending on the stress regime by plotting b-values versus rake angles (indicating slip direction of the hanging wall) for a large variety of earthquakes. For a b-value less than 1, the vertical stress is the least principal compressive stress and we are in a thrust-fault regime. If the vertical stress is intermediate, the b-value will likely be around 1, indicating a strike-slip faulting regime. And if it exceeds 1, then the stress regime is extensional, with the maximum principal stress vertical, creating a normal fault regime.

The case study of Grob and Van der Baan (2011) using a microseismic dataset recorded over a heavy oil field drained using cyclic steam stimulation revealed that the in situ stress state changed from extensional to compressive with an intermediate strike-slip regime, indicating initial opening and then closing of fractures. This occurred over an 8-month period where pure injection in the first four months was followed by combined injection and production in different parts of the field (Figure 4). We postulate that analysis of the statistical b-values will provide complementary information to temporal and spatial variations in the in situ stress field as determined by moment-tensors inversions, and therefore contains a wealth of information to facilitate reservoir management.

5.3. Relating geomechanical properties to microseismic observables

Various observations suggest that microseismic events tend to occur preferentially in specific lithologies only (e.g., a sand) but not in some others (e.g., a shale), even if fluids are known to traverse both lithologies in a hydraulic fracturing experiment, shown in Figure 5 (Rutledge et al., 2004, Pettitt et al., 2009). This suggests that deformation in some rock types may occur aseismically, especially in higher-permeability, ductile shales, or simply that the radiated elastic energy for microseismic events in some rock types may occur at frequencies that are too low to be detected using conventional recording systems. Moreover, anecdotal information suggests that the abundance and intensity of microseismic events may not necessarily correlate to the effectiveness of the fracture treatments (Maxwell et al., 2008; Boroumand and Eaton, 2012).

The concept of microseismic efficiency represents the ratio of radiated seismic energy (Vassiliou and Kanamori, 1982) to the total deformation energy. Analysis of deformation energy is being done by using pressure, rate, fluid/proppant volume and other relevant data curves produced from the surface equipment in order to calculate the total energy/work produced to generate fractures in the ground. Often substantial differences are estimated between the total input energy inferred from fluid injection rates and pressures, the fracture

http://dx.doi.org/10.5772/56444

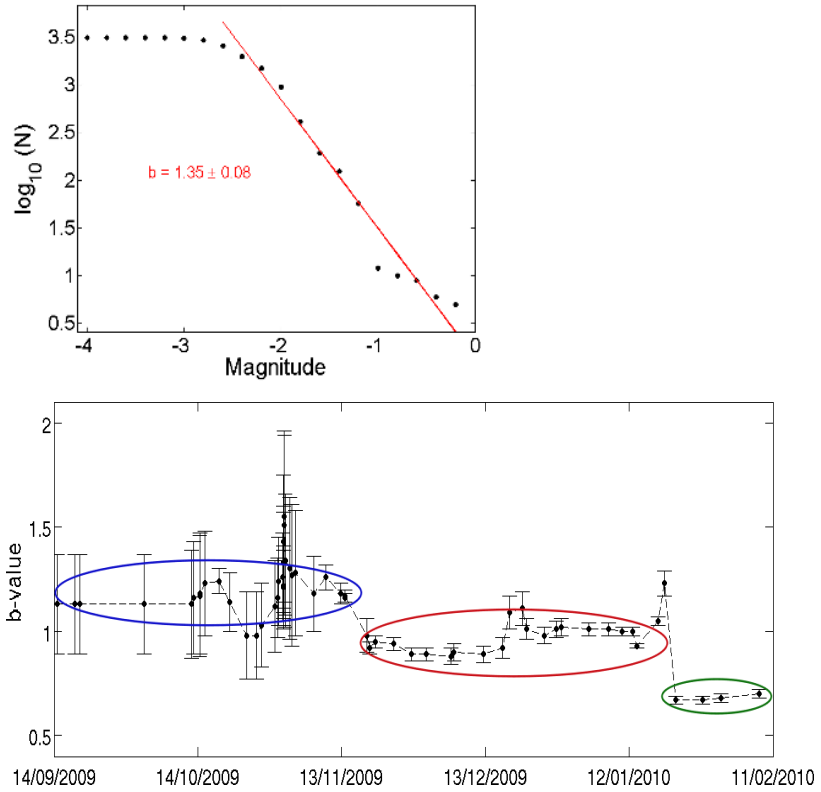

Figure 4. Analysis of frequency-magnitude variations in microseismic events recorded over a heavy-oil field drained using cyclic-steam stimulation (after Grob and Van der Baan, 2011). Top: Distribution of event sizes for the whole dataset. Shown is the cumulative number of events smaller than a given magnitude. A fit on the linear part of the curve gives a b-value of 1.35 indicating overall extensional faulting. Bottom: Temporal evolution of b-values for this dataset. Three stages are visible: at the beginning high b-values larger than 1.0 (implying extensional faulting or opening of fractures) until November 2009, followed by b-values around 1.0 and finally a last stage with values around 0.65 (indicating closing of fractures or compressive faulting), starting end of January 2010. Pure steam injection took place prior to November 2009, followed by a combined injection and production in different parts of the field. The statistical analysis of frequency-magnitude variations in microseismic data provide us with invaluable information on changes in the underlying stress fields.

energy to pry apart the walls of a single very large fracture, and the radiated energy observed from recorded seismicity. The injected energy is 10^4–10^7 times larger than the estimated radiated seismic energy, and the fracture energy is inferred to be 15–40% of the input energy (Maxwell et al., 2008; Boroumand and Eaton, 2012).

The three most likely factors to dominate the geomechanical behavior of a reservoir are the local in situ stress regime, pre-existing fractures (and other zones of weaknesses), and the actual rock properties (e.g., whether they are more ductile or brittle as expressed by their Young's modulus or Poisson's ratio and thus the Lamé parameters). In order to better understand why

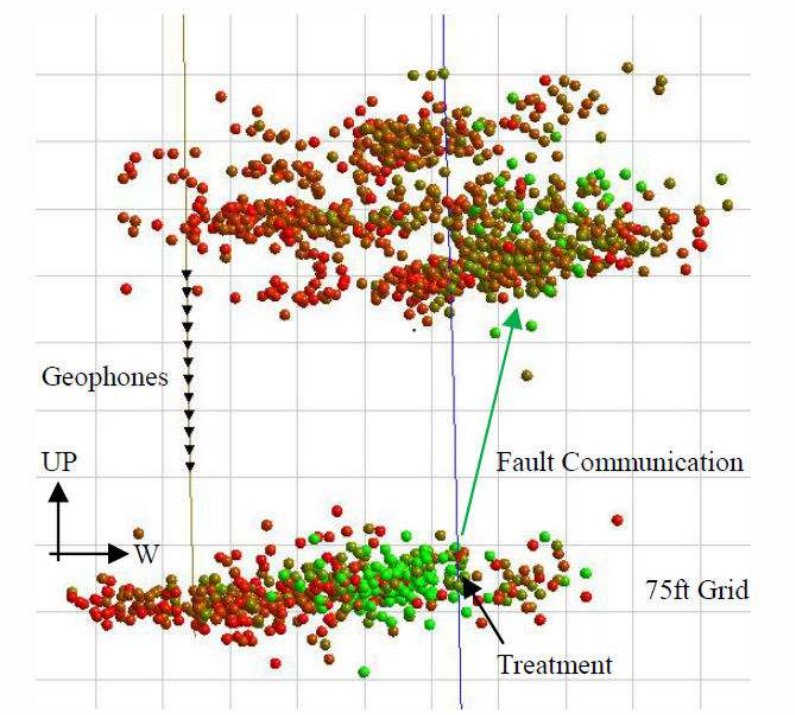

Figure 5. Hydraulic fracturing of a tight-gas sand. 1408 events are recorded over 5 hours. Events are colour shaded by time: green (earliest) to red (latest). Events occur in two formations with very few detected events in between. Yet the event history reveals that brittle failure occurs first in the right-most part of the bottom formation, and then suddenly jumps to the top formation indicating the presence of a possible aseismic fault. After Pettitt et al. (2009).

the seismic efficiency is so low, and what precisely happens when we are injecting fluids at high pressures into rocks we need to improve our understanding of what the various geophysical observations (moment tensors, hypocentres, resonance frequencies, etc.) truly reveal of the newly induced fracture networks specifically, and the geomechanical reservoir response in general. Three general options to achieve this objective are analogues, computational modelling, and physical modelling in the laboratory.

5.4. Analogues

Dusseault et al. (2011) use analogues to explain many of the fracturing processes that may occur when fluids and/or proppants are injected at high pressure into intact and naturally fractured rock. They consider a medium composed of rigid blocks and injection of a solid. This leads to many insights despite the fact that this is clearly a great simplification of reality.

In Figure 6 a solid material is injected into a material composed of rigid blocks, producing tensile mode I fracturing (i.e., wedging) at the tips of the proppant inclusions, and mode II (i.e.,

http://dx.doi.org/10.5772/56444

shearing) in the surrounding areas due to block rotations. Wedging creates fracture openings well beyond the proppant tips (or infiltration extents) due to normal extensional forces on the surfaces of the joint leading to tensile (mode I) failure and facilitating slurry/proppant penetration. It also leads to a large increase in the effective permeability in a zone beyond the proppant infiltration.

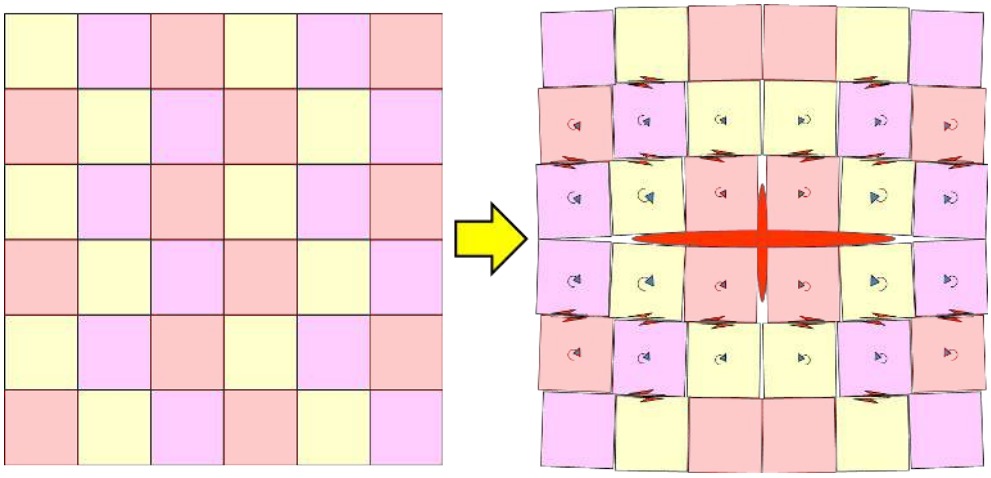

Figure 6. Analogues can help us understand how fluid and/or proppant injection into a reservoir zone affects the resulting rock deformation. In this case a solid material is injected into a material comprised of rigid blocks, showing clearly where propping, wedging, rotation and shearing will occur. Such observations provide important clues on the anticipated moment tensors throughout the resulting microseismic event cloud. From: Dusseault et al. (2011).

Block rotation continues beyond the area of proppant infiltration and tensile opening at the proppant tips. It involves large changes in both the normal and shear forces excited on the joint surfaces, yielding predominantly mode II fracturing (i.e., shearing). This may cause slip on existing joints in naturally fractured rocks, and even facilitate fault reactivation if the effective stresses are sufficiently to close to criticality. Shear displacement along natural fractures is associated with self-propping where irregular joint surfaces after slip create remnant apertures, facilitating subsequent fluid flow (Dusseault et al., 2011). Such observations provide important clues on the anticipated moment tensors throughout the resulting microseismic event cloud, demonstrating that tensile source mechanism are likely to dominate close to the proppant tips, but double-couple events in all other areas.

Obviously fluid and/or proppant infiltration into naturally fractured rock is significantly more complex since the exact behaviour will depend on the situ stress field, pre-existing in natural fractures and lithologies. The interaction of brittle failure in intact rock and the slip/shearing in naturally fractured areas can be complex (Figure 7); yet the principles deduced from the study of analogues should help unravel the various competing processes.

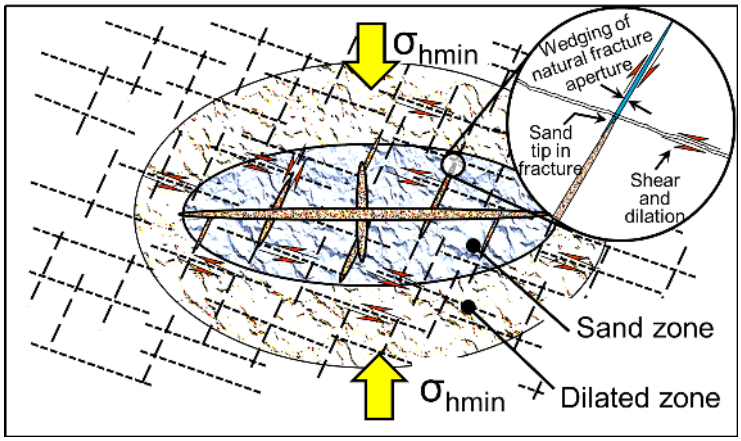

Figure 7. Fluid and/or proppant injection into a reservoir zone will create new fractures, as well as close, shear or pop open existing fractures. The various failure mechanisms may lead to a larger microseismic cloud surrounding the area of injected fluids, thereby improving reservoir drainage. The microseismic events are therefore also characterized by a variety of earthquake mechanisms. Their analysis can yield a wealth of knowledge on the underlying failure mechanisms beyond mere locations. From: Dusseault et al. (2011).

5.5. Geomechanical modelling

Analogues provide a first understanding on how fluid and/or proppant injection is likely to deform the surrounding rock mass (Figures 6 and 7). They also provide pertinent clues on where to expect brittle failure (and thus microseismic events) and their most probable failure mechanism (source mechanism). Geomechanical modeling is subsequently a great aid for improving our understanding on links between fluid-induced rock failure, the occurrence of microseismicity and underlying geomechanical behaviour, beyond the assumption of rigid blocks and no fluid diffusion (i.e., no leak off).

Bonded-particle modeling is becoming an important computational tool for modeling the complex dynamical behavior of rocks rupturing given a set of boundary conditions (Potyondy and Cundall, 2004). This approach simulates rock deformation using an assemblage of rigid, round particles that are bonded together. This grid of particles can deform freely and bonds can be broken to represent local failure. Bonds are characterized by normal and shear strengths as well as friction coefficients to model respectively tensile and shear failure. Such a discontinuum-based approach seems more appropriate to model rock deformation through failure since it eliminates the need for complex constitute relations required for continuum approaches (Hazzard and Young, 2000). Also microseismic moment tensors can be inferred by integrating local bond failure in both space and time (Hazzard and Young, 2004).

Chorney et al. (2012) use bonded-particle modelling to examine resulting seismicity for triaxial compression tests using different confining pressures. The resulting Hudson plots (i.e., moment-tensor distribution) show a surprising similarity with those obtained for real data by

http://dx.doi.org/10.5772/56444

Baig and Urbancic (2010) from field observations of hydraulic fracturing (Figure 8). Baig and Urbancic (2010) find dominant failure mechanisms of double couple (shearing) and fracture opening and closing (tensile failure and closing). This confirms insights gained from the analogues (Figures 6 and 7) where shearing and tensile failure seem to dominate, respectively, in the surrounding area and at the tips of the proppant infiltrations.

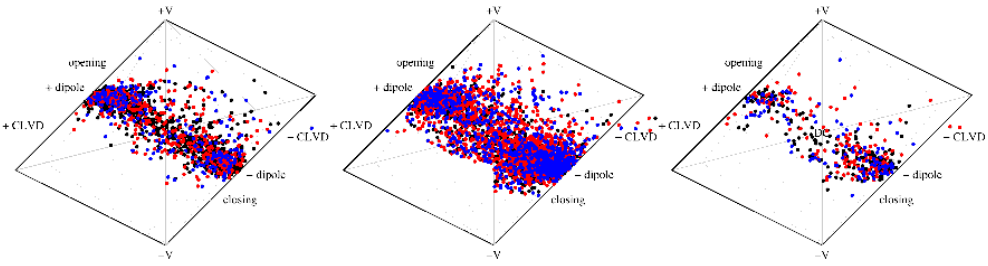

Figure 8. Hudson plots of the failure mechanisms for microseismic events in the bonded-particle simulations for triaxial compression tests with confining pressures of 0 MPa (left) and 40 MPa (right). The colors represent the time: pre-peak stress events are in black; events happening around peak stress are in red and post-peak events are displayed in blue (modified from Chorney et al., 2012). Both fracture opening and closing (tensile failure and closing) occurs. CLVD: Compensated-linear vector dipole. The simulated seismicity shows a surprising correspondence with real field measurements from hydraulic fracturing experiments (e.g., Baig and Urbancic, 2010).

Chorney et al. (2012) also monitor the total input energy of the system, the total kinetic energy emitted from bond breakages, and the energy deduced from the moment magnitudes of the microseismic events. The kinetic energy represents approximately 5% of the input energy; the radiated seismic energy is 50-100 times smaller than the kinetic energy. The radiated energy calculated using the Gutenberg-Richter relationship between moment magnitude and energy may thus underestimate the energy incurred from brittle failure. Both the radiated and kinetic energy from brittle failure are substantially lower than the input energy. This confirms observations by Maxwell et al. (2009) and Boroumand and Eaton (2012). Ductile or slow, aseismic deformation must thus constitute a significant term in the energy budget for both these numerical simulations of triaxial compression and for hydraulic fracturing experiments in general.

Approaches such as bonded-particle models are thus useful to study the anticipated geomechanical behavior of a reservoir; in particular anticipated brittle failure (as expressed by a microseismic event) as well as any aseismic deformation (due to semi-brittle or plastic flow). Ultimately, they may help to investigate how resulting deformation and microseismic emissions depend on (1) in the in situ stress regime, which relates to the magnitude and ratio of the vertical stress Sv and the maximum and minimum horizontal stresses SH and Sh; (2) pre-existing fractures and other zones of weakness most likely to break; and finally (3) the local rock properties defined by the Young's modulus and Poisson's ratio (both related to the Lamé parameters). Constraints on many of these factors can be obtained using the processing and interpretation techniques described previously.

Unfortunately, discontinuum-based methods such as bonded-particle approaches may be less suitable to simulate fluid injection as fluids can only be described as small particles.

Continuum-based approaches such as finite-element methods may be required for coupled fluid-flow and geomechanical simulation (Dean et al., 2003; Minkoff et al., 2003; Angus et al., 2010). On the other hand, particle-based methods are highly appropriate to modelling crack propagation and brittle failure. Although this is feasible with continuum-based approaches it leads to highly expensive computations. Angus et al. (2010), for instance, circumvent the requirement for modelling fracture propagation by assuming that the differential effective stress tensor at the local point of failure is a first-order approximation to the local failure mechanism (Zoback and Zoback, 1980). For failure in intact rock this is likely a reasonable assumption, but not for failure along pre-existing weaknesses (Gephart and Forsyth, 1984).

5.6. Physical modelling

Ultimately physical modelling in the laboratory is required to confirm our inferences from the study of analogues and numerical simulations, thereby completing the circle between fluid-induced rock failure, the occurrence of microseismicity and underlying geomechanical deformation. Many authors have studied the links between microseismic event locations and fracture growth in both triaxial compression and hydraulic fracturing tests (Solberg et al., 1980; Sondergeld and Estey, 1981; Kranz et al., 1990; Lockner et al., 1991; Lockner, 1993; Chitrala et al., 2010). Most of these studies were successful in determining the event hypocenters; yet few provided reliable full moment tensor solutions. The latter are essential for better understanding the actual rock failure mechanisms.

The analogues are very useful for building a first understanding on what to expect when injecting fluids and/or proppants into the rock matrix (Figures 6 and 7) but the combination of numerical simulations and their verification using physical experiments in the laboratory will help to bridge the gap between geophysical data analysis and engineering applications of microseismic data by providing a framework for advanced interpretation strategies, thereby facilitating completion of the the circle between acquisition, processing and interpretation.

6. Conclusions

The recent surge in development of unconventional resources such as shale-gas and heavy-oil plays has created renewed interest in microseismic monitoring. Pore pressure and stress changes during fluid and/or proppant injection lead to an expanding cloud of microseismic events, due to brittle failure in intact rock and additional slip/shearing in naturally fractured rock. The microseismic cloud represents thus a volumetric map of the extent of induced fracture shearing and opening; yet integration of event locations with moment tensors, other geophysical observations and geomechanical constraints is required to determine ultimately the size of the interconnected fracture network, thereby excluding isolated fracturing/shearing, since only the former contributes to the enhanced effective porosity and permeability, required for predicting actual reservoir drainage.

http://dx.doi.org/10.5772/56444

Due to a strong desire for near-real time information by completion engineers, acquisition and service companies have focused predominantly on providing hypocentre locations and moment magnitudes. Microseismic recordings contain, however, a wealth of information beyond event locations, including moment tensors and resonance frequencies. Thus, many pertinent research questions on microseismic acquisition, processing and interpretation remain to be answered before full use of microseismic recordings can be achieved.

Nonetheless, microseismic monitoring has a bright future with long-standing applications such as monitoring of shaft stability in mines and the creation of engineered geothermal systems; more recent applications involve monitoring of hydraulic stimulation of "tight" hydrocarbon reservoirs and steam-injection in heavy-oil fields. Future applications may incorporate surveillance of CO_2 storage as well as slurried waste solids disposal through continuous injection.

Acknowledgements

The first two authors would like to thank the sponsors of the Microseismic Industry Consortium for financial support. Arc Resources, Nanometrics and ESG Solutions are particularly thanked for their support of the field project. All authors would like to thank their collaborators, students and postdocs whose work has contributed tremendously to this paper.

Author details

Mirko van der Baan[1], David Eaton[2] and Maurice Dusseault[3]

*Address all correspondence to: Mirko.vanderBaan@ualberta.ca

1 University of Alberta, Edmonton, Alberta, Canada

2 University of Calgary, Calgary, Alberta, Canada

3 University of Waterloo, Waterloo, Ontario, Canada

References

[1] Aki, K., Fehler, M., and Das, S., 1977, Source mechanism of volcanic tremors: fluid-driven crack model and their application to the 1963 Kilauea eruption: Journal of Volcanology and Geothermal Research, 2, 259–287.

[2] Albright, J. N., and Pearson, C. F., 1982. Acoustic emissions as a tool for hydraulic fracture location: experience at the Fenton Hill Hot Dry Rock site: Soc. Petr. Eng. Journal., 22: 523-530.

[3] Angus D. A., J.-M. Kendall, Q.J. Fisher, J.M. Segura, S. Skachkov, A.J.L. Crook and M. Dutko, 2010, Modelling microseismicity of a producing reservoir from coupled fluid-flow and geomechanical simulation: Geophysical Prospecting, 58, 901–914.

[4] Arrowsmith S. J. and Eisner L., 2006, A technique for identifying microseismic multiplets and ap-plication to the Valhall field, North Sea, Geophysics, 71 (2), V31 – V40.

[5] Baig, A. and Urbancic, T., 2010. Microseismic moment tensors: A path to understanding frac growth. The Leading Edge, 29: 320-324.

[6] Ben-Menahem, A. and S.J. Singh (2000). Seismic Waves and Sources. 2nd edition, Dover Publications, New York.

[7] Benson, P. M., S. Vinciguerra, P. G. Meredith, and R. P. Young, 2008, Laboratory simulation of volcano seismicity: Science, 322, 249–252.

[8] Beroza, G.C. and Ide, S. 2011. Slow earthquakes and nonvolcanic tremor. Annual review of Earth and planetary sciences, 39: 271-296.

[9] Beroza, G.C. and Satoshi, I. 2011. Slow earthquakes and nonvolcanic tremor. Annual review of Earth and planetary sciences, 39: 271-296.

[10] Bolt, B.A., 1984. Inside the Earth : evidence from earthquakes. W.H. Freeman, 191 pp.

[11] Boroumand, N., and D. W. Eaton, 2012, Comparing Energy Calculations - Hydraulic Fracturing and Microseismic Monitoring: 74th Mtg., EAGE, Copenhagen, C042.

[12] Brown, A., 2004, Interpretation of three-dimensional seismic data. American Association of Petroleum Geologists; 6th edition, 560 pp.

[13] Brune, J. N., 1970. Tectonic stress and the spectra of seismic shear waves from earthquakes. J. Geophys Res., 75: 4997-5009.

[14] Brune, J.N., 1971. Correction. J. Geophys. Res., 76: 5002.

[15] Castellanos F. and Van der Baan M. (2012) High-accuracy relative event locations using a combined multiplet analysis and the double-difference inversion. 82nd Ann. Int. Mtg., SEG, Las Vegas, PSC4.

[16] Chambers, K., Kendall, J. M., Dahl, S.B., and Rueda, J., 2009. The detectability of microseismic events using surface arrays: EAGE Workshop on Passive Seismic Limassol, Cyprus.

[17] Chitrala, Y., C. Moreno, C. Sondergeld and C. Rai, 2011, Microseismic and microscopic analysis of laboratory induced hydraulic fractures. SPE 147321.

http://dx.doi.org/10.5772/56444

[18] Chorney, D., Jain, P., Grob, M. and van der Baan, M., 2012, Geomechanical modeling of rock fracturing and associated microseismicity: The Leading Edge, 31, N. 11, 1348-1354.

[19] Clarkson, C.R., Aguilera, R., Pedersen, P.K., and Spencer, R.J., 2011. Shale gas, part 8: Shale gas development optimization. CSPG Reservoir, 38(4): 25-31.

[20] Cypster, D.A. and Davis, S.D., 1998. Induced seismicity and the potential for liability under U.S. law. Tectonophysics, 289: 239-255.

[21] Das, I. and Zoback, M.D., 2011. Long-period, long-duration seismic events during hydraulic fracture stimulation of a shale gas reservoir. Leading Edge, 30: 778-786.

[22] De Meersman K., Kendall J-M. and Van der Baan M. 2009. The 1998 Valhall microseismicity: An integrated study of relocated sources, seismic multiplets and S-wave splitting. Geophysics, 74(5), B183-B195.

[23] de Pater, H. & Baisch, S., 2011, Geomechanical Study of Bowland Shale Seismicity, Synthesis Report, commissioned for Cuadrilla resources, accessed online http://www.cuadrillaresources.com/wp-content/uploads/2012/02/Geomechanical-Study-of-Bowland-Shale-Seismicity_02-11-11.pdf

[24] de Ridder, S. and Dellinger, J., 2011. Ambient seismic noise eikonal tomography for near-surface imaging at Valhall. Leading Edge, 30: 506-512.

[25] Dean R.H., Gai X., Stone C.M. and Minkoff S.E. 2003. A comparison of techniques for coupling porous flow and geomechanics. SPE Reservoir Simulation Symposium, 3–5 February, Houston, Texas, USA, Expanded Abstracts, 79709.

[26] Dusseault M., J. McLennan and S. Jiang (2011) Massive multi-stage hydraulic fracturing for oil and gas recovery from low mobility reservoirs in China: Petroleum Drilling Techniques, 39 (3), 6-16.

[27] Eaton, D.W., 2011. Q determination, corner frequency and spectral characteristics of microseismicity induced by hydraulic fracturing. SEG Annual Meeting, San Antonio, Abstract PSC 3.4 .

[28] Eaton D. (2012) Crack-tip Stress Field, Coulomb Failure, and the Spectral Characteristics of Tensile Rupture. 74th EAGE Conference & Exhibition incorporating SPE EUROPEC 2012, Copenhagen, Denmark.

[29] Eaton, W.D., Akram, J., St-Onge, A., and Forouhideh, F., 2011. Determining microseismic event locations by semblance-weighted stacking: CSPG CSEG CWLS Convention, Calgary.

[30] Eaton, D.W. and Forouhideh, F., 2010. Microseismic moment tensors: The good, the bad and the ugly. CSEG Recorder, 35(9), 45-49.

[31] Eaton, D.W. and Forouhideh, F., 2011. Solid angles and the impact of receiver-array geometry on microseismic moment-tensor inversion. Geophysics, 76: WC75-WC83.

[32] EIA (Energy Information Administration), 2011. International Energy Outlook 2011, DOE/EIA-0404, 301 pp. Accessed online at http://www.eia.gov/forecasts/ieo/pdf/0484(2011).pdf.

[33] Eisner L., Duncan P., Heigl W., and Keller W., 2009. Uncertainties in passive seismic monitoring: The Leading Edge, 28: 648-655.

[34] Ferrazzini, V., and Aki, K., 1987, Slow waves trapped in a fluid-filled infinite crack: implication for volcanic tremor, Journal of Geophysical Research, 92(B9), 9215-9223.

[35] Fu, Q., and Luo, Y., 2009, Locating Micro-Seismic Epicenters in Common Arrival Time Domain: SEG Houston International Exposition and Annual Meeting, 1647-1651.

[36] Gajewski, D., 2005. Reverse modelling for seismic event characterization: Geophysical Journal International, 163: 276–284.

[37] Gephart J. and Forsyth D. 1984. An improved method for determining the regional stress tensor using earthquake focal mechanism data: Application to the San Fernando earthquake sequence. Journal of Geophysical Research B11, 9305–9320.

[38] Gibowicz , S. and Kijko, A., 1994. An introduction to mining seismology. Academic Press, 399 pp.

[39] Got, J.-L., 1994, Deep fault plane geometry inferred from multiplet relative relocation beneath the south flank of Kilauea: Journal of Geophysical Research, 99, 15375–15386.

[40] Grob, M. and van der Baan, M., 2011, Inferring in-situ stress changes by statistical analysis of microseismic event characteristics: The Leading Edge, 30, no. 11, p. 1296–1301.

[41] Han, L., Wong, J., and Bancroft, J., 2009. Time picking and random noise reduction on microseismic data: CREWES Research Report, 21, 1-13.

[42] Han, L., 2010, Microseismic Monitoring and Hypocentre Location: MS Thesis, University of Calgary.

[43] Häring, M.O., Schanz, U., Ladner, F. and Dyer, B.C., 2008. Characterisation of the Basel 1 enhanced geothermal system. Geothermics, 37: 469–495.

[44] Hazzard JF, Young RP., 2000. Simulating acoustic emissions in bonded-particle models of rock: International Journal of Rock Mechanics and Mining Sciences, 37(5), 867–872.

[45] Hazzard JF, Young RP., 2004. Dynamic modeling of induced seismicity: International Journal of Rock Mechanics and Mining Sciences, 41, 1365–1376.

[46] Hudson, J., Pearce, R. and Roberts, R., 1989. Source type plot for inversion of the moment tensor. J. Geophys. Res., 94: 765-774.

http://dx.doi.org/10.5772/56444

[47] Ide, S., Beroza, G.C., Shelly, D.R. & Uchide, T. (2007) A scaling law for slow earthquakes. Nature 447, 76-79.

[48] IHS CERA, 2010, Fueling North America's Energy Future, Executive Summary, 12 pp. Accessed at http://www2.cera.com/docs/Executive_Summary.pdf.

[49] Jones, G. A., Raymer, D., Chambers, K., and Kendall, J. M., 2010. Improved microseismic event location by inclusion of a priori dip particle motion: a case study from Ekofisk: Geophysical prospecting, 58: 727-737.

[50] Karpfinger, F., 2009, Modelling borehole wave signatures in elastic and poroelastic media with spectral method, Ph. D. Thesis, Curtin University of Technology, Aus.

[51] King, G. E. (2012) Hydraulic Fracturing 101: What Every Representative, Environmentalist, Regulator, Reporter, Investor, University Researcher, Neighbor and Engineer Should Know About Estimating Frac Risk and Improving Frac Performance in Unconventional Gas and Oil Wells. SPE 152596.

[52] Kocon K. and Van der Baan M. (2012) Quality assessment of microseismic event locations and traveltime picks using a multiplet analysis. The Leading Edge, 31(11), 1330-1337. Kranz, R. L., T. Satoh, O. Nishizawa, K. Kusunose, M. Takahashi, K. Masuda, A. Hirata, Laboratory study of fluid pressure diffusion in rock using acoustic emissions, J. Geophys. Res., 95, 21593–21607, 1990.

[53] Lamb, H., 1917. On waves in an elastic plate, Proceedings of the Royal Society, London: 114-128.

[54] Lockner, D. A., 1993, The role of acoustic emission in the study of rock fracture. lnt. J. Rock Mech. Min. Sci. & Geomech. Abstr. Vol.30, No.7, pp. 883-899.

[55] Lockner, D.A., J. D. Byerlee, V. Kuksenko, A. Ponomarev and A. Sideron, 1991, Quasi-static fault growth and shear fracture energy in granite: Nature, 350, 39-42.

[56] Madariaga, R., 1977. High frequency radiation from cracks (stress drop) models of earthquake faulting. Geophys. J., 51: 625-652.

[57] Maxwell, S.C., 2010. Microseismic: growth born from success. Leading Edge, 29: 338-343.

[58] Maxwell, S.C., 2011. Microseismic hydraulic fracture imaging; the path toward optimizing shale gas production. Leading Edge, 30: 340-346.

[59] Maxwell, S.C., Shemata, J., Campbell, E., and Quirk, D., 2008, Microseismic deformation rate monitoring. SPE 116596.

[60] Maxwell, S.C., Shemeta, J., Campbell, E., and Quirk, D., 2009. Microseismic deformation rate monitoring", EAGE, A18.

[61] Maxwell, S. C., C. K. Waltman, N. R. Warpinski, M. J. Mayerhofer, and N. Boroumand, Imaging seismic deformation induced by hydraulic fracture complexity, SPE paper 102801.

[62] Maxwell, S.C., Rutledge, J., Jones, R. and Fehler, M.C. 2010. Petroleum reservoir characterization using downhole microseismic monitoring. Geophysics, 75: 75A129-75A137.

[63] McGillivray, P., 2005, Microseismic and time-lapse seismic monitoring of a heavy oil extraction process at Peace River, Canada: CSEG Recorder, 30(1): 5-9.

[64] Michaud, G., Leslie, D., Drew, J., Endo, T., and Tezuka, K., 2004. Microseismic event localization and characterization in a limited aperture HFM experiment: SEG International Exposition and 74th Annual Meeting, Denver Colorado.

[65] Minkoff S.E., Stone C.M., Bryant S., PeszynskaM. and Wheeler M.F. 2003. Coupled fluid flow and geomechanical deformation modelling. Journal of Petroleum Science and Engineering 38, 37–56.

[66] Oye, V., and Roth, M., 2003. Automated seismic event location for hydrocarbon reservoirs: Computers & Geosciences, 29, 851 – 863.

[67] Pettitt W., J. Reyes-Montes, B. Hemmings, E. Hughes and R. P. Young, 2009, Using continuous microseismic records for hydrofracture diagnostics and mechanics: SEG, Expanded Abstracts, 28, 1542-1546.

[68] Potyondy DO, Cundall PA., 2004. A bonded-particle model for rock: International Journal of Rock Mechanics and Mining Science, 41(8):1329–64.

[69] Poupinet G, Ellsworth W, Frechet J, 1984, Monitoring velocity variations in the crust using earthquake doublets: An application to the Calaveras fault, California: J. Geophys. Res., 89, 5719–5731. Raggio, L., Etcheverry, J., and Bonadeo, N., 2007. Determination of acoustic shear and compressional wave velocities for steel samples by impulse excitation of vibrations, IV Conferencia Panimericana de END, Buenos Aires.

[70] Reine C., M. Van der Baan and R. Clark (2009) The robustness of seismic attenuation measurements using fixed- and variable-window time-frequency transforms: Geophysics, 74(2), WA123-WA135.

[71] Rutledge, J.T., W. S. Phillips, and M. J. Mayerhofer, 2004, Faulting induced by forced fluid injection and fluid flow forced by faulting: An interpretation of hydraulic fracture microseismicity, Car-thage Cotton Valley gas field, Texas: Bulletin of the Seismological Society of America, 94, 1817–1830.

[72] Schorlemmer, D., Wiemer, S. and Wyss, M., 2005, Variations in earthquake-size distribution across different stress regimes, Nature, 437, 539-542, doi:10.1038/nature04094.

[73] Sharma, B.K., Kumar, A., and Murthy, V.M., 2010. Evaluation of seismic event-detection algorithms: Journal geological society of India, 75, 533 - 538.

[74] Shearer, P., 1999, Introduction to seismology, Cambridge University Press.

[75] Shemata, J. and Anderson, P., 2010. It's a matter of size: Magnitude and moment estimates for microseismic data. Leading Edge, 29: 296-302.

[76] Solberg, P. H., Lockner, D. A., and Byerlee, J. D., 1980, Hydraulic fracturing in granite under geothermal conditions, International J. of Rock Mech., v. 17, p. 25-33.

[77] Sondergeld, C. H., L. H. Estey, 1981, Acoustic emission study of microfracturing during the cyclic loading of Westerly Granite, J. Geophys. Res., 86, 2915–2924.

[78] Stein, S. and Wysession, M., 2003. An introduction to seismology, earthquakes, and earth structure. Blackwell, 498 pp.

[79] St-Onge, A. and Eaton, D., 2011. Noise examples from two microseismic datasets. CSEG Recorder, 6(8): 46-49.

[80] Sun, R., and McMechan, G., 1988, Finite-Difference Modeling of Borehole Resonances: Energy Resources, 10, 55-75.

[81] Tary, J., and van der Baan, M., 2012, Potential use of resonance frequencies in microseismic interpretation, The Leading Edge, 31, 1338-1346.

[82] Tary, J., and van der Baan, M., 2013, On the interpretation of resonance frequencies recorded during microseismic experiments, 2013 Geoconvention, Calgary, submitted.

[83] Teanby, N., J.-M. Kendall, R. Jones, and O. Barkved, 2004a, Stress-induced temporal variations in seismic anisotropy observed in microseismic data: Geophysical Journal International, 156, 459–466.

[84] Teanby N.A., Kendall J-M. and Van der Baan M. (2004b) Automation of shear-wave splitting measurements using cluster analysis. Bull. Seism. Soc. Am., 94, 453-463.

[85] Thompson, B. D., R. P. Young, and D. A. Lockner, 2009, Premonitory acoustic emissions and stick-slip in natural and smooth-faulted Westerly granite, Journal of Geophysical Research, 114, B02205.

[86] Urbancic, T. and Trifu, C., 2000. Recent advances in seismic monitoring technology at Canadian mines. Journal of Applied Geophysics, 45: 225-237.

[87] Vassiliou, M.S. and Kanamori, H., 1982. The energy release in earthquakes. Bull. Seismol. Soc. Am., 72: 371-387.

[88] van der Baan, M., 2009, The origin of SH-wave resonance frequencies in sedimentary layers, Geophysical Journal International, 178, 1587-1596.

[89] van der Baan, M., Wookey, J., and Smit, D., 2007, Stratigraphic filtering and source penetration depth, Geophysical Prospecting, 55, 679-684.

[90] Verdon, J.P, Kendall, J-M, White, D.J., Angus, D.A., Fisher, Q.J. and Urbancic, T., 2010. Passive seismic monitoring of carbon dioxide storage at Weyburn. Leading Edge, 29, 200-206.

[91] Waldhauser, F., and Ellsworth, W. L., 2000, A Double-Difference Earthquake Location Algorithm: Method and Application to the Northern Hayward Fault, California: Bull. Seis. Soc. Am., 90, 1353-1368.

[92] Walter, W.R. and Brune, J.N., 1993. Spectra of seismic radiation from a tensile crack. J. Geophys. Res., 98: 4449-4459.

[93] Warpinski, N., 2009. Microseismic Monitoring: Inside and Out. Journal of Petroleum Technology, 61(11), 80-85.

[94] Xuan, R., and Sava, P., 2009. Probabilistic micro-earthquake location for reservoir monitoring: SEG Houston International Exposition and Annual Meeting: 1637-1641.

[95] Zoback M. and Zoback M. 1980. State of stress in the conterminous United States. Journal of Geophysical Research 85, 6113–6156.